

Modeling the heat flux and wind turbulence in Lake Tanganyika

Student: Libin Zhang

Mentor: Jim Russell

INTRODUCTION

The heat flux and the wind driven turbulence in Lake Tanganyika can be more thoroughly understood through theoretical modeling. This study models the energy flux balance of Lake Tanganyika to predict changes in water temperature due to air temperature changes, and also models wind-driven turbulence, upwelling, and stratification, providing information pertinent to more complex modeling. Turbulent kinetic energy accumulation, predictable from wind stress and the lake's temperature profile, may sometimes provide enough work to induce destratification. Calculations correlated with empirical data show that sustained wind speeds over 5 m/s cause upwelling of the thermocline. Wind-induced waves also transport sediments down the water column, with stronger winds transporting larger grain sizes; a more simplified formula is provided for the depth to which various grain sizes are transported by different wind speeds. Future work coupling thermocline mixing with nutrient upwelling should provide insight into biological productivity.

THE MODELS

Energy Flux

The net energy flux of a lake is a summation of the constituent energy fluxes: solar shortwave radiation, ϕ_{sw} , atmospheric longwave radiation ϕ_{lw} , back longwave radiation from the lake surface ϕ_{lu} , and latent q_{latent} and sensible $q_{sensible}$ heat fluxes from the lake.

$$\phi_{sw} + \phi_{lw} - \phi_{lu} - q_{latent} - q_{sensible} \quad [W/m^2]$$

Each term can be calculated from theoretical grounds, using the input parameters of surface water temperature T_w [$^{\circ}C$], (dry) air surface temperature T_a [$^{\circ}C$], wind speed, cloud cover, solar radiation, and relative humidity (Figure 1).

Solar shortwave radiation ϕ_{sw} [W/m^2] is the amount of solar radiation that is absorbed by the lake surface. Earth-bound radiometers record shortwave solar radiation that passed through the clouds, with an additional fraction (albedo) of the radiation being reflected. Water albedo can diurnally vary from 0.03 to 0.3; an average albedo of 0.06, used for oceans (1), is used for the lake.

All bodies with temperatures above absolute zero radiate heat energy, including the atmosphere. This *atmospheric longwave radiation* ϕ_{lw} [W/m^2] is defined as (2)

$$\phi_{lw} = \epsilon_{air} \sigma_{SB} (T_a + 273.15 \text{ K})^4 (1 + 0.17 C_{cover}^2)$$

where α_{lw} is the longwave albedo, ϵ_{air} is the emissivity of air, σ_{SB} is the Stephan-Boltzmann constant [$5.67 \times 10^{-8} \text{ W m}^{-2} \text{ K}^{-4}$], and C_{cover} is the cloud cover as a fraction. Since longwave is less reflective than shortwave radiation, it is assumed that longwave albedo is half (0.03) shortwave albedo.

McIntyre 2002 (2) defines the emissivity of air using T_a and air vapor pressure e_a [kPa]

$$\epsilon_{air} = 0.642 \left(\frac{1000 e_a}{T_a + 273.15 \text{ K}} \right)^{1/7}$$

Back longwave radiation from the lake surface ϕ_{lu} [W/m^2] is similar to atmospheric longwave radiation, with the emissivity of water (ϵ_{water}) = 0.97 (3):

$$\phi_{lu} = \epsilon_{water} \sigma_{SB} (T_w + 273.15 \text{ K})^4$$

Evaporation changes the lake's *latent heat flux* [W/m^2], given by the following equation (4, 5):

$$q_{latent} = [b_o (T_w - T_a)^{1/3} + L_v N_{mt} W_2] (e_o - e_a) \quad (6)$$

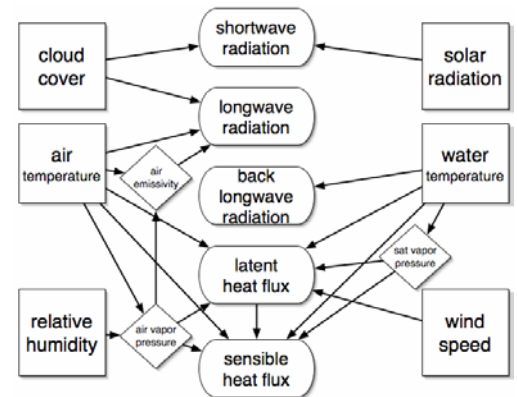


Figure 1. Diagram shows model inputs (in squares) and model outputs (in ovals).

$b_0 = 27 \text{ W m}^{-2} \text{ kPa}^{-1} \text{ } ^\circ\text{C}^{1/3}$, L_v is the latent heat of vaporization [J/kg], N_{mt} is the mass-transfer coefficient, and W_2 is the wind speed [m/s] at 2 meters above the lake surface. The saturated and air vapor pressures, e_0 and e_a , are in kPa.

The mass-transfer coefficient is defined as a function of lake area A_{lake} [$3.26 * 10^{10} \text{ m}^2$] (4, 7)

$$N_{mt} = 3.367 * 10^{-5} A_{\text{lake}}^{-0.05}$$

Saturated vapor pressure e_0 [kPa] is approximated by a common equation (8)

$$e_0 = 0.6108 \text{ kPa } e^{17.27 T_a / (T_a + 237.3)}$$

Air vapor pressure e_a [kPa] uses the same formula as saturated vapor pressure, except T_w is substituted for T_a and the result is multiplied by the decimal equivalent of relative humidity (4).

Heat lost from the water surface by convection and conduction is termed sensible heat loss. The *sensible heat flux* is calculated by multiplying the latent heat flux by a Bowen ratio (4)

$$Q_{\text{sensible}} = R_{\text{Bowen}} Q_{\text{latent}} = Q_{\text{latent}} \gamma_p \frac{(T_w - T_a)}{(e_0 - e_a)}$$

The psychrometric constant γ_p [kPa K^{-1}] (9) is based on T_a and surface air pressure P [$\approx 92.5 \text{ kPa}$] (10)

$$\gamma_p = 0.000660 (1 + 0.00115 T_a) * P$$

A summation of all the energy flux terms to generate a net energy flux, which is assumed to be close to zero or steady-state, will allow the evaluation of the effects of changes in input parameters on the output energy fluxes.

Wind-driven turbulence and mixing

Wind stress and wind-driven cooling in Lake Tanganyika contribute to upwelling (13). Wind introduces turbulent kinetic energy to the lake by creating a wind stress τ_0 [N/m^2] on the lake surface. The stress is difficult to measure, so it is commonly parameterized using wind speed. The wind stress generates a friction velocity u_* [m/s] (14)

$$\tau_0 = \rho_{\text{air}} C_{10} W_{10}^2$$

$$u_* = (\tau_0 / \rho)^{1/2}$$

ρ_{air} is the density of air [kg/m^3], C_{10} is the drag (or wind stress) coefficient, and W_{10} [m/s] is the wind speed 10 meters above the surface. The drag coefficient is not constant, as the coupling between air and water depends on surface roughness (15). $C_{10} \approx 0.001$ for $W < 7 \text{ m/s}$, and then it increases steadily until $C_{10} \approx 0.0025$ for $W > 17\text{-}20 \text{ m/s}$.

The *turbulent kinetic energy* (TKE) [W/kg] in the water column associated with wind-driven turbulence is calculated by

$$\text{TKE} = \frac{1.8 u_*^3}{k_{\text{karman}} h} = 1.8 \left(\frac{\rho_{\text{air}} C_{10}}{\rho} \right)^{3/2} \frac{W_{10}^3}{k_{\text{karman}} h}$$

k_{karman} is the von Karman constant [≈ 0.41], and the constant 1.8 is empirically determined (16). Above the depth at which this turbulent kinetic energy is significant sediment can be mobilized and below it stratification is induced. The accumulation of TKE can also translate into work used for upwelling.

Sediment transport

Increasingly strong wind-induced surface waves influence the transport of coarse-grained sediment at increasing depths due to the downward transport of turbulent kinetic energy. The maximum size of the sediment grains capable of being transported by a wave can serve as a proxy for the strength of wave influence.

Table 1. Basic Physical Properties of Air and Water

Surface water density ρ_0 [kg/m^3] (11) is based on water temperature T ($^\circ\text{C}$)

$$\rho_0(T) = 999.843 + 10^{-3} (65.49 T - 8.563 T^2 + 0.05939 T^3)$$

and on conductivity: $\rho_0(T, \kappa_{20}) = \rho_0(T) [1 + \beta_k \kappa_{20}]$

κ_{20} is the conductivity at 20°C [$\mu\text{S/cm}$] and $\beta_k = 0.705 * 10^{-6} (\mu\text{S/cm})^{-1}$.

The density of water changes with depth (12) $\rho^P = \rho^0 (1 - P/K)^{-1}$

P is water pressure [bar] and K [bar] is a variable based on T and P .

$$K = 19652.17 \text{ bar} + 148.113 T - 2.293 T^2 + 1.256 * 10^{-2} T^3 - 4.18 * 10^{-5} T^4 + (3.2726 - 2.147 * 10^{-4} T + 1.128 * 10^{-4} T^2) P$$

For $T = 20 - 30^\circ\text{C}$, the thermal coefficient of expansion α [K^{-1}] is (2)

$$\alpha = 1.6 * 10^{-5} + 9.6 * 10^{-6} T$$

The density of air varies with temperature and air vapor pressure

$$\rho_{\text{air}} = 1.2929 \text{ kg m}^{-3} \left(\frac{273.15 \text{ K}}{T_{\text{air}} + 273.15 \text{ K}} \right) \left(\frac{94 \text{ kPa} - 0.3783 e_a}{101.325 \text{ kPa}} \right)$$

Water's latent heat of vaporization [J/kg] is dependent on T (8)

$$L_v = 2.501 * 10^6 - 2361 T_w$$

For waves of uniform size in deep water, the Sverdrup-Munk-Metschneider (SMB) Method (17) can derive wave length L [m], wave period T [s], and wave height H [m], from water depth h_o [m] and wind speed W [m/s]. The latter is the mean wind speed measured 8 m above the lake surface (18).

$$H_{\infty} = \frac{a W^2}{g} 0.283 \operatorname{Tanh} \left[\frac{0.125}{a} \left(\frac{g F}{W^2} \right)^{0.42} \right] \quad \text{where } a = \operatorname{Tanh} \left[0.53 \left(\frac{g h_o}{W^2} \right)^{0.75} \right]$$

$$T_{\infty} = \frac{2 \pi b W}{g} 1.2 \operatorname{Tanh} \left[\frac{0.077}{b} \left(\frac{g F}{W^2} \right)^{0.25} \right] \quad \text{where } b = \operatorname{Tanh} \left[0.833 \left(\frac{g h_o}{W^2} \right)^{0.375} \right]$$

$$L_{\infty} = \frac{g T^2}{2 \pi} \operatorname{Tanh} \left[\frac{2 \pi h_o}{L_{\infty}} \right] \quad (L_{\infty} \text{ must be calculated iteratively})$$

g is the gravitational acceleration [9.81 m s^{-2}] and F is the lake's effective fetch, which is a measure of the distance over which the winds may act upon the waves. For Lake Tanganyika, the effective fetch is assumed to be lake length, or 650 000 m, as the rift valley tends to channel winds along the length of the rift axis.

Changes occur in the wave geometries as the waves approach shallower waters. While T remains constant ($T = T_{\infty}$), L and H change to near-shore values that depend on water depth h [m]

$$L = L_{\infty} \left(\operatorname{Tanh} \left[\frac{2 \pi h}{L_{\infty}} \right] \right)^2$$

$$H = H_{\infty} \sqrt{\frac{L_{\infty}}{L} \left(1 + \frac{2 k h}{\sinh [2 k h]} \right)^{-1}} \quad \text{where } k = \frac{2 \pi}{L_{\infty}}$$

The waves create orbital motions that entrain sandy sediments (19, 20). The elliptical water motion at a given depth h [m] has a horizontal displacement l_n [m] and a maximum horizontal velocity u_m [m/s].

$$l_n = H / \sinh \left[\frac{2 \pi h}{L} \right] \quad \text{and} \quad u_m = \frac{\pi l_n}{T}$$

An empirical relationship between wave motion and sediment grain size (d) [m] moved by the passing wave, for grains smaller than 0.5 mm (21), has been determined

$$d = \left(\frac{\rho * u_m^2}{0.13 (\rho_s - \rho) g \sqrt{l_n}} \right)^2$$

Given a grain size d , one can solve for the maximum depth that a given wind velocity will transport the grains.

METHODS

Data sources

Meteorological parameters from the period March 1993 through December 1995 are taken from Table 13 of Verburg et al. 1997 (10). The table contains data from meteorological stations at Mpulungu, Bujumbura, and Kigoma, as well as two buoys at Mpulungu and Kigoma. The stations and buoys recorded such parameters as wind speed and gust, air and water temperature, relative humidity, and solar radiation. The two buoys provided monthly average water temperature profiles down to 300 meters depth. The Kigoma Airport meteorologist provided long-term cloud cover data, from 1994 to 1997, used for the Kigoma energy flux model (Figure 2). Kigoma/Bujumbura represents the north end of the Lake while Mpulungu represents the south end.

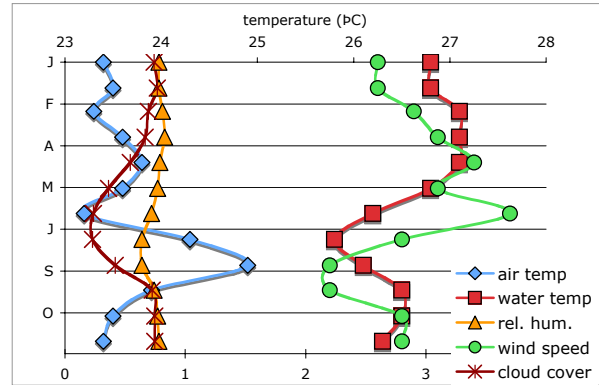


Figure 2. Monthly average of five input model parameters for Kigoma (solar radiation input not shown). Air and water temperature use the *top x-axis* [$^{\circ}\text{C}$]. Relative humidity (rel. hum.) [fraction], wind speed [m/s], and cloud cover [fraction] use the *bottom x-axis*.

Several water profiles were taken by a Hydrolab Datasonde 4a at Kitwe Point, Nondwa Point, and off the Luiche River near Kigoma in July 2005. The Hydrolab records temperature, conductivity, pH, and dissolved oxygen concentration every ten seconds, up to 200 meters depth. The first temperature profile, taken at Kitwe Point on July 24, 2005, is representative of subsequent results and is used for water column modeling (Figure 3). The Kitwe thermocline starts at 65 m, while the Nondwa thermocline starts at 60 m.

Physical calculations

Energy Flux: The various weather parameters are combined to create an energy flux model using the equations in the introduction, with the annual net energy flux as close to zero as possible. To estimate the effects of surface warming of Africa due to anthropogenic global climate change on Lake Tanganyika, the monthly average air temperature is uniformly increased incrementally, to examine the changes in the different component energy fluxes. The surface water temperature is subsequently uniformly raised until the air-temperature-induced energy flux increase is balanced.

Water column: The water column temperature profile from Kitwe Point is used to calculate turbulent kinetic energy (TKE) at several different wind speeds. Real monthly wind speed and gust data (10) are used to calculate TKE down the water column at Mpulungu and Kigoma, as well as total TKE each month. It is assumed that wind speed is constant between two meters and ten meters above ground.

Sediment transport: A relationship is first established theoretically between wind gust and the depth to which grains of different sizes are transported using the SMB method. Real monthly wind gust data is used to calculate what size grains are transported to what depths at Kigoma and Mpulungu.

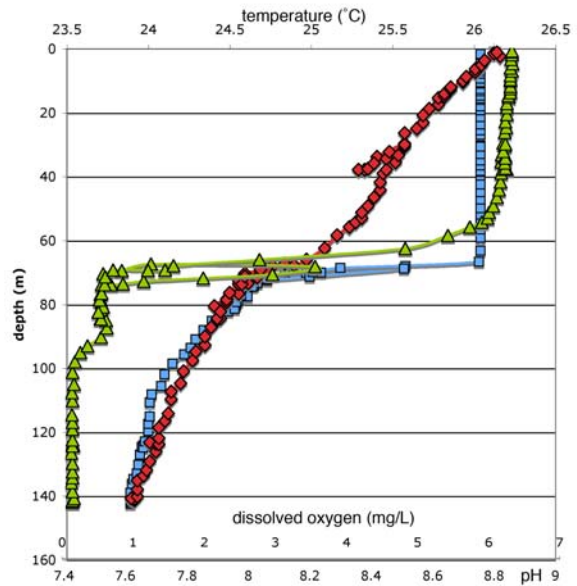


Figure 3. Temperature [$^{\circ}\text{C}$] (blue squares), dissolved oxygen [mg/L] (green triangles) and pH (red diamonds) with depth at Kitwe Point, July 23, 2005, 10 AM. The pH may have been miscalibrated, but the pH is not used in modeling.

RESULTS

Energy Flux

The energy flux from the lake surface at Kigoma is almost perfectly balanced, with a net annual energy flux of negative 19.1 W/m^2 (Figure 4(a)). Back longwave radiation slightly exceeds longwave radiation due to the higher water temperature than air temperature; the greatest sources of inter-monthly variations are the heat fluxes. The net annual flux is unbalanced at Mpulungu (potential annual loss of 400 W/m^2 , Figure 4(b)) perhaps due to the lack of data on cloud cover from that region. The annual loss may also be indicative of real heat loss in southern parts of the Lake.

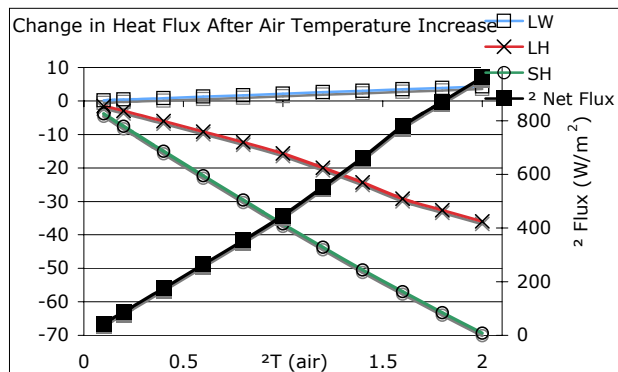


Figure 5. Right y-axis: Increases in Kigoma air temperature, ΔT (air), cause a positive change in net annual heat flux.

Left y-axis: Changes in the total annual longwave flux (LW), latent heat flux (LH), and sensible heat flux (SH) due to ΔT (air).

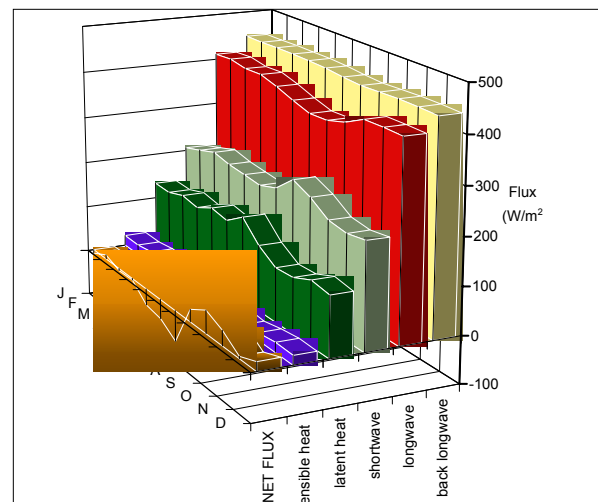
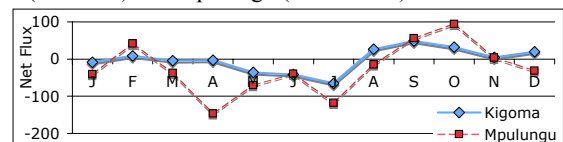


Figure 4. Above (a). Monthly energy fluxes in Kigoma. **Below (b).** Monthly net energy fluxes at Kigoma (balanced) and Mpulungu (unbalanced).



Small artificial changes in air temperature cause dramatic increases in net energy flux (+500 W/m² per °C, *Figure 5 right axis*). All the other input parameters are kept constant. The flux increase is entirely due to a small percentage increase in the longwave radiation, with offsetting decreases in latent heat and sensible heat fluxes (*Figure 5 left axis*). All the other energy fluxes remain unchanged in the model.

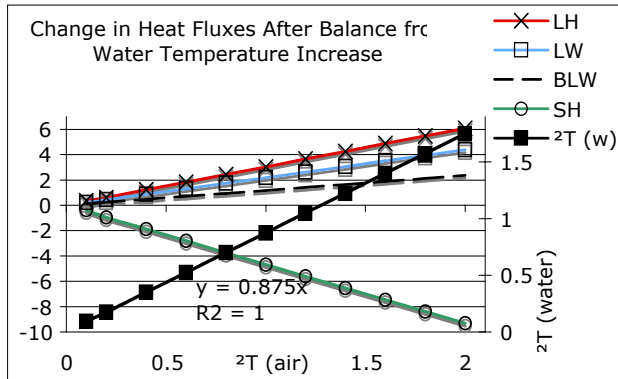


Figure 6. Right y-axis: An increase in water temperature, ΔT (water), is needed to restore the heat flux balance after ΔT (air). The correlation between the two ΔT is almost perfectly linear.

Left y-axis: The final resulting deviance in LW, BLW (Back Longwave), LH, and SH fluxes after the overall net flux has been balanced by the increase in water temperature.

The lake's net energy flux is restored to the original value of negative 19.1 W/m² by an increase in water temperature that exhibits the relationship $\Delta T_{\text{water}} = 0.875 \Delta T_{\text{air}}$ ($R^2 = 1$, *Figure 6 right axis*). The restored energy flux comes mostly from increasing back longwave radiation. The latent heat flux actually *increases*, while the sensible heat flux decreases by a small amount (*Figure 6 left axis*).

Given a range of future water surface temperature increases, it would be nice to be able to infer temperatures further down the water column. However, the correlations between surface temperatures and temperatures at depth are very weak (*Figure 12 in the Discussion section*).

Monthly turbulent kinetic energy

Using the water temperature profile from Kitwe Point, turbulent kinetic energy (TKE) decreases exponentially down the water column (*Figure 7*). The gradual accumulation of TKE leads to an increasingly unstable water column.

Mpulungu has high TKE in the summer and autumn months (*Figure 8 (d)*), which corresponds to periods of strong upwelling (*Figure 8(c)*). The TKE for Kigoma (*Figure 8(b)*) is lower than at Mpulungu, correlating with a more stable water column (*Figure 8(a)*). A more quantitative relationship between TKE and upwelling can be evaluated through determining the energy required for upwelling.

The work W_s [J m⁻²] needed to fully destratify a water column up depth z_m is (22, 23):

$$W_s = \frac{g}{A_{\text{lake}}} \int_0^{z_m} (z - z_{<\rho>}) (\rho_z - <\rho>) A_z dz$$

where $<\rho>$ is the mean water density [kg m⁻³], $z_{<\rho>}$ is the depth [m] at $<\rho>$, ρ_z is the density at each depth z , and A_z and A_{lake} are the area of the lake at depth z and at the surface, respectively.

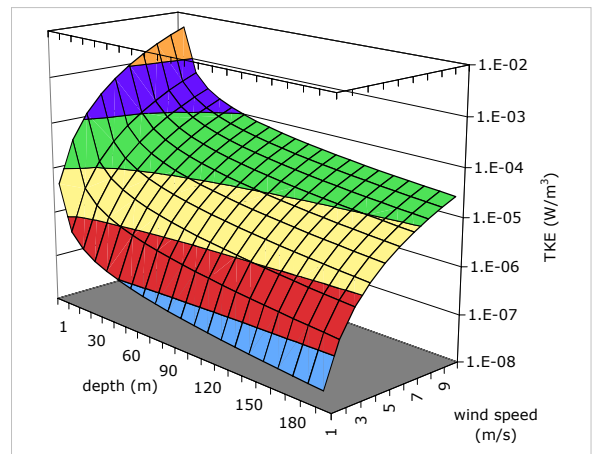


Figure 7. Theoretical Relationship Between Turbulent Kinetic Energy (TKE), wind speed, and water depth. Each color band corresponds to a different TKE order of magnitude. Note the logarithmic scale.

Assuming that $A_{\text{lake}} = A_z$, the work required to destratify up to $z_m = 200$ m of the Kitwe water column ($z_{<\rho>} = 85.6$ m, $\langle\rho\rangle = 997.57 \text{ kg m}^{-3}$) is $W_s = 56.0 \text{ kJ/m}^2$.

TKE accumulates over time; when it exceeds W_s , it is possible that water is sufficiently energetic for destratification. The relationship between days required for $\text{TKE} = W_s$ and wind speed (W) is inversely cubic ($\text{Days} = 4879 W^{-3}$, $R^2 = 1.000$, plot not shown). At Mpulungu, either twelve days of gust winds or forty days of average winds are required for destratification (Figure 9), which are reasonable time spans (24). The time periods should be considered overestimations, as the real water column is never fully destratified with uniform water density. TKE accumulation is not sufficient to induce upwelling at Kigoma.

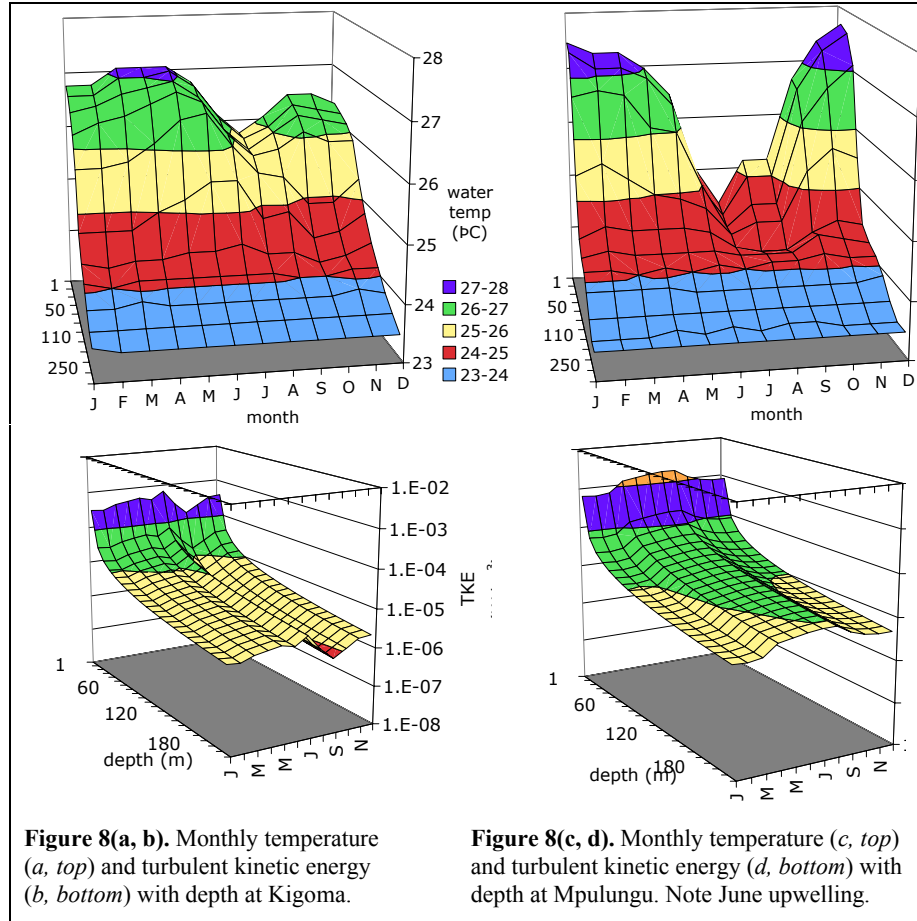


Figure 8(a, b). Monthly temperature (a, top) and turbulent kinetic energy (b, bottom) with depth at Kigoma.

Figure 8(c, d). Monthly temperature (c, top) and turbulent kinetic energy (d, bottom) with depth at Mpulungu. Note June upwelling.

Wind transport of sediments

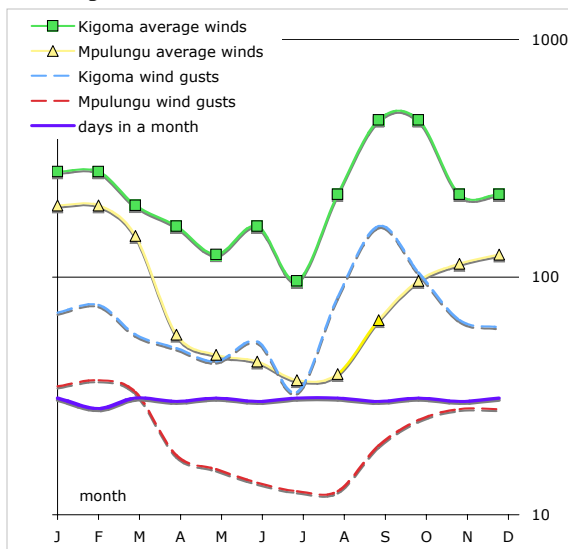


Figure 9. Logarithmic plot showing the number of days required for total kinetic energy (TKE), from average winds or wind gusts at Kigoma and Mpulungu, to equal destratification work W_s .

Theoretical SMB sediment transport calculations show that stronger winds transport smaller grain sizes deeper down the water column in a quadratic relationship (Figure 10).

Using the 1993-1995 wind gust data for Kigoma and Mpulungu, aragonite grains ($d = 2.86 \mu\text{m}$ (25)) are predicted to be absent in Kigoma above 15 meters and in Mpulungu above 25 meters (Figure 11). Aragonite has not been found in Luiche Platform and Tafiri Bay at depths shallower than 20 meters (25), which corresponds to wind gusts around 6 m/s, a speed that reasonably could have occurred in the last ten years.

Some basic assumptions can lead to major simplification of the sediment transport equations. Assuming that h_0 is large and $L/L_\infty \approx H/H_\infty \approx 1$, the sediment grain size equations can be simplified to produce a direct relationship between water depth h [m] and grain size d [m]

$$h = \frac{1.44 W^2 a^2}{g} \text{ArcSinh} \left[\text{Tanh} \left[0.0125 \left(\frac{F g}{W^2} \right)^{0.42} \right] \right] / \sqrt[3]{\frac{24.7384 d g (\rho - \rho_s)^2}{W^2 \rho^2} a^4}$$

$$a = \text{Tanh} \left[0.077 \left(\frac{F g}{W^2} \right)^{1/4} \right]$$

the simpler equations above deviate < 4% from the truer, more complex values of water depth h for $W \geq 2$ m/s.

Wind turbulence vs. Convective turbulence

Wind turbulence is not the sole agent for thermocline waters mixing into the well-mixed surface layer h_{mix} ; another source is convective turbulence. The relative importance of wind vs. convective turbulence changes with depth. Convective turbulence is quantified by the *surface buoyancy flux* J_b^0 [W/kg] that arises from the rate of change of density, $d\rho/dt$, in h_{mix} due to evaporation (14). It is defined with the specific heat of water c_p [4181.2 J kg⁻¹ K⁻¹] and net heat flux H_{net} ($= -(q_{\text{latent}} + q_{\text{sensible}})$)

$$J_b^0 = - \frac{\alpha g}{C_p \rho} H_{\text{net}}$$

The depth at which J_b^0 equals TKE is known as the

Monin-Obukhov Length L_m [m], $L_m = \frac{-u_*^3}{k J_b^0}$. If the Monin-Obukhov Length is shallower than the well-mixed surface layer h_{mix} , the major contribution to entrainment and mixing at the bottom of the surface layer is convection. If $L_m > h_{\text{mix}}$, wind is the major contributor.

L_m at Kigoma and Mpulungu ranges between 1.6 and 5.8 m (Figure 11). Since L_m is much less than $h_{\text{mix}} = 60-65$ m, convective turbulence plays a greater entrainment role in much of the surface mixed layer. The disparity between the strong influence of TKE accumulation with the weak role of wind-driven turbulence in comparison to convective turbulence is a source of debate.

DISCUSSION AND CONCLUSION

Model predictions

For every 1 °C increase in surface air temperature, surface water temperature will increase by 0.875 °C to maintain energy flux balance. Unfortunately, it is not possible to extrapolate any water temperature changes further down the water column. Linear regressions on historical water column temperature profiles (26-31) show no strong relationship between an increase in surface water temperatures and increase in bottom water temperatures. The strongest regression is a negative correlation between the temperatures at surface and 200 m depth (Figure 12), which possibly arises because water warming is raising the thermocline. If it is assumed that surface water rises in temperature but bottom waters do not, and that the intermediate temperatures rise proportionately, then the work necessary for destratification rises W_s [kJ/m²] = 11.72 $\Delta T_{\text{watersurface}} + 55.89$ ($R^2 = 0.9999$) and the days before destratification with wind speed W ,

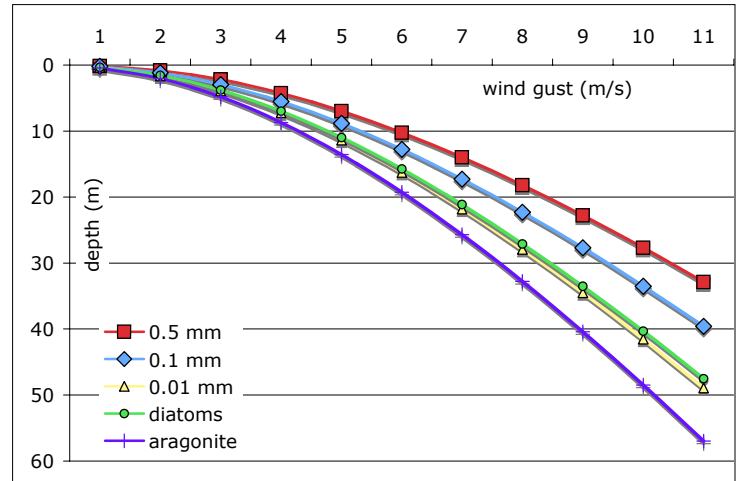


Figure 10. Maximum depths to which different grain sizes are transported by wind gusts. All grains have $\rho = 2.6$ g/cm³, except for diatoms. Aragonite $d = 2.86$ μm . Diatoms $d = 0.03$ mm, $\rho = 2.1$ g/cm³.

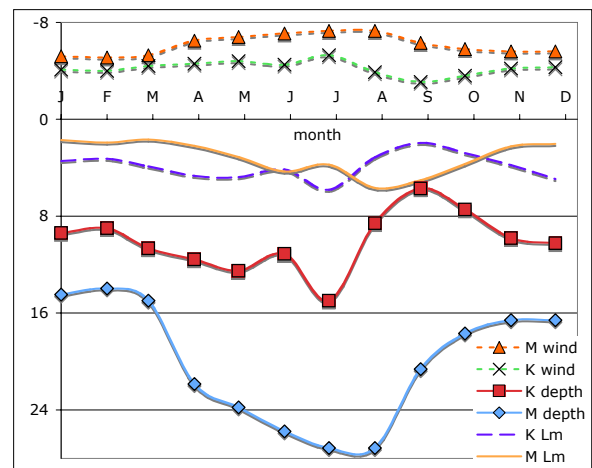


Figure 11. Wind gusts, depths to which aragonite grains are transported, and Monin-Obukhov Lengths (L_m) at Mpulungu (M) and Kigoma (K).

Days = $(4870 + 1020 \Delta T_{\text{watersurface}}) W^{-3}$. The predictions are qualitatively in concurrence with previous Lake Tanganyika studies on the effects of global climate change (27).

Theoretical calculations show that a monthly wind speed of 5.5 m/s would accumulate enough turbulent kinetic energy to exceed the work needed for destratification to 200 m after 30 days. Since the water column is never fully destratified, even sustained lower wind speeds will be enough to induce upwelling. Having more wind data and temperature profiles, especially during periods of upwelling, will allow stronger prediction confirmation.

The Monin-Obukhov Lengths are lower than the depth of the well-mixed surface layer, implying that convective turbulence is more significant than wind-driven turbulence. However, surface buoyancy flux and thus convective turbulence remain relatively constant over time and with depth (32); wind contributes additional, variable energy for destratification work.

Future research

Much additional work remains to be done for modeling Lake Tanganyika. Although the theoretical underpinnings of the models are solid, more recent and comprehensive limnologic and climatic datasets would provide stronger input parameters and more empirical confirmation of model predictions. In particular, reliable wind speed and gust information over the lake and over all time scales would be very useful in studying model sensitivity. Cloud cover information for the southern end of the lake, or an equation correlating cloud cover with clear sky shortwave radiation, would be highly useful in modeling the southern energy flux.

The models make many basic assumptions and simplifications. Various other forms of lake mixing have been ignored, such as internal waves (13), seiches, Langmuir cells (33, 34), eddy diffusivity, Kelvin-Helmholtz instabilities (35), boundary mixing (14), and so on. Numbers that parameterize lake stability, such as the Brunt-Väisälä frequency and the Gradient Richardson Number, were calculated but not used. A future two-dimensional model of the lake will need to incorporate the north-south gradient of the lake, rather than simply examine two sites at Kigoma and Mpulungu.

A better understanding of the lake physics may eventually lead to predictions about upwelling rates and biological productivity (27, 36). A relatively simple task is to look at the amount of nutrient upwelling expected during destratification to predict the biomass changes at various trophic levels.

ACKNOWLEDGEMENTS

I would like to acknowledge the palaeoclimatology mentor J. Russell, the palaeoclimatology TA L. Powers, and the limnology mentor C. O'Reilly. I would also like to thank those with me on the *Echo* to collect Hydrolab data: S. Close, A. Kiviyiro, Chata and Chale. This work was financed by the Nyanza Project (NSF ATM-0223920).

REFERENCES

1. J. Knauss, "Chapter 4: The transfer of heat across the ocean surfaces" in *Introduction to Physical Oceanography (Second Edition)*. (Prentice-Hall, Upper Saddle River, New Jersey, 1997) pp. 39-58.
2. S. McIntyre, J. Romero, G. Kling, Spatial-temporal variability in surface layer deepening and lateral advection in an embayment of Lake Victoria, East Africa. *Limnol. Oceanogr.* **47** (3), 656-71 (2002).
3. E. R. Anderson, Energy budget studies, water loss investigations - Lake Hefner studies. *U.S. Geol. Surv. Prof. Paper* **269**, 71 (1954).

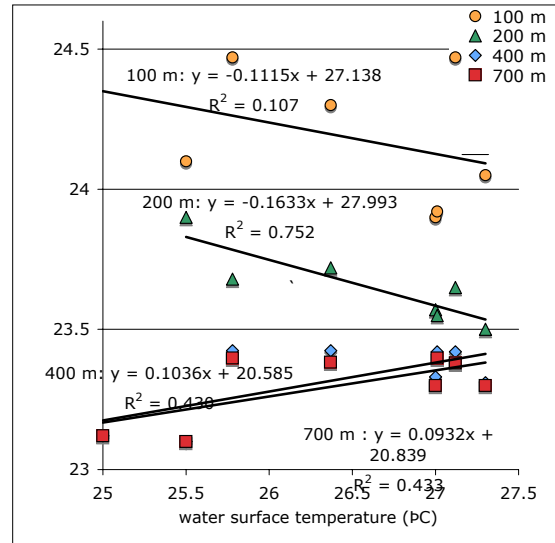


Figure 12. Empirical regressions between surface water temperature and temperature at various depths (100, 200, 400, 700 m). The lack of positive correlation is evident.

4. S. W. Hostetler, "Chapter 3: Hydrological and thermal response of lakes to climate description and modeling" in *Physics and Chemistry of Lakes (Second Edition)* A. Lerman, D. M. Imboden, J. R. Gat, Eds. (Springer-Verlag, Berlin Heidelberg, 1995) pp. 63-82.
5. P. J. Ryan, D. R. F. Harleman, K. D. Stolzenbach, Surface heat loss from cooling ponds. *Water Resour. Res.* **10**, 930-8 (1974).
6. Hostetler has T_w and T_a in virtual temperature form, which accounts for humidity, but the difference is not significant.
7. W. Brutsaert, *Evaporation into the atmosphere* (Reidel, Dordrecht, 1982), pp. 299.
8. R. L. Snyder, Humidity Conversion. <http://biomet.ucdavis.edu/conversions/HumCon.htm> (March 24, 2005).
9. L. J. Fritschen, L. W. Gray, *Environmental Instrumentation* (Springer-Verlag, New York, NY, 1979), pp.?
10. T. H. P. Verburg, B. Kakogozo, A. Kihakwi, P. Kotilainen, L. Makasa, A. Peltonen, "Hydrodynamics of Lake Tanganyika and Meteorological Results" (Finnish International Development Agency, February 1997).
11. H. Buhner, H. Ambühl, Die Einleitung von gereinigtem Abwasser in Seem. *Schweiz. Z. Hydrol.* **37**, 347-69 (1975).
12. C. T. Chen, F. J. Millero, Precise thermodynamic properties for natural waters covering only the limnological range. *Limnol. Oceanogr.* **31** (3), 657-62 (1986).
13. G. W. Coulter, R. H. M. S. Spigel, "Chapter 3: Hydrodynamics" in *Lake Tanganyika and its Life* G. W. Coulter, Ed. (Oxford University Press, Oxford, 1991) pp. 49-75.
14. D. M. Imboden, A. Wüest, "Chapter 4: Mixing Mechanisms in Lakes" in *Physics and Chemistry of Lakes (Second Edition)* A. Lerman, D. M. Imboden, J. R. Gat, Eds. (Springer-Verlag, Berlin Heidelberg, 1995) pp. 83-138.
15. J. Amorochio, J. J. deVries, A new evaluation of the wind stress coefficient over water surfaces. *J. Geophys. Res.* **85**, 433-42 (1980).
16. C. P. Lombardo, M. C. Gregg, Similarity scaling of e and x in a convecting surface boundary layer. *J. Geophys. Res.* **94**, 6273-84 (1989).
17. T. C. Johnson, "Sediment redistribution by waves in lakes, reservoirs and embayments", presented at the Symposium on Surface Water Impoundments ASCE, Minneapolis, Minnesota, June 2-5 1980.
18. L. J. Håkanson, M., *Principles of Lake Sedimentology* (Springer-Verlag, Berlin Heidelberg, 1983), pp. 177-93.
19. P. D. Komar, M. C. Miller, The threshold of sediment movement under oscillatory water waves. *J. Sediment. Petrol.* **43**, 1101-10 (1973).
20. P. D. Komar, M. C. Miller, On the comparison between the threshold of sediment motion under waves and unidirectional currents with a discussion of the practical evaluation of the threshold. *J. Sediment. Petrol.* **45**, 362-7 (1975).
21. R. W. Sternberg, L. H. Larsen, Threshold of sediment movement by open ocean waves: observations. *Deep-Sea Res.* **22**, 299-309 (1975).
22. S. B. Idso, On the concept of lake stability. *Limnol. Oceanogr.* **18** (4), 681-3 (1973).
23. W. Schmidt, Über Temperatur und Stabilitätsverhältnisse von Seen. *Geogr. Ann.* **10**, 145-77 (1928).
24. C. M. O'Reilly, personal communication (2005).
25. G. Jimenez, personal communication (2005).
26. L. Van Meel, "Contribution à la Limnologie de Quatre Grands Lacs du Zaire Oriental: Tanganyika, Kivu, Mobutu Sese Seko (ex Albert), Idi Amin Dada (ex Edouard). Les Paramètres Chimiques, Fascicule A: Le Lac Tanganyika" (Institut Royal des Sciences Naturelles de Belgique, Brussels, Belgium, 1987).
27. C. M. O'Reilly, S. R. Alin, P.-D. Plisnier, A. S. Cohen, B. A. McKee, Climate change decreases aquatic ecosystem productivity of Lake Tanganyika, Africa. *Nature* **424** (2003).
28. H. Marquardsen, Die Seen Tanganjika. Meoro und Bangweolo. *Mitteilungen aus den Deutschen Schutzgebieten Berlin* **29**, 97-8 (1916).
29. J. M. Edmond, Nutrient chemistry of the water column of Lake Tanganyika. *Limnol. Oceanogr.* **38**, 725-38 (1993).
30. H. Craig, "Lake Tanganyika Geochemical and Hydrographic Study: 1973 Expedition" (Univ. California San Diego, 1974).
31. R. S. A. Beauchamp, Hydrology of Lake Tanganyika. *Internationale Revue der Gesamten Hydrologie und Hydrographie* **39**, 316-53 (1939).
32. From calculations: Kigoma surface buoyancy flux range 0.68 – 1.3, standard deviation 1.4 [10^{-7} W/kg]. Mpulungu surface buoyancy flux range 2.2 – 6.1, standard deviation 0.96 [10^{-7} W/kg].
33. I. Langmuir, Surface motion of water induced by wind. *Science* **87**, 119-23 (1938).
34. S. Leibovich, The form and dynamics of Langmuir circulations. *Annu. Rev. Fluid Mech.* **15**, 391-427 (1983).
35. J. D. Woods, Wave-induced shear instability in the summer thermocline. *J. Fluid Mech.* **32**, 791-800 (1968).
36. R. E. Hecky, R. H. Spigel, G. W. Coulter, "Chapter 4: The nutrient regime" in *Lake Tanganyika and its Life* G. W. Coulter, Ed. (Oxford University Press, Oxford, 1991) pp. 76-89.